Deregulated Myc Requires MondoA/Mlx for Metabolic Reprogramming and Tumorigenesis

Patrick A. Carroll[1,#], **Daniel Diolaiti**[1,#], **Lisa McFerrin**[1], **Haiwei Gu**[2], **Danijel Djukovic**[2], **Jianhai Du**[4], **Pei Feng Cheng**[1], **Sarah Anderson**[1], **Michelle Ulrich**[1], **James B. Hurley**[4,5], **Daniel Raftery**[2,3], **Donald E. Ayer**[6], and **Robert N. Eisenman**[1,*]

[1]Division of Basic Sciences, Fred Hutchinson Cancer Research Center, MS A2-025, P.O. Box 19024, Seattle, WA, 98109-1024

[2]Northwest Metabolomics Research Center, Department of Anesthesiology and Pain Medicine, University of Washington, 850 Republican St, Room S148, P.O. Box 358057, Seattle, WA 98109-8057

[3]Division of Public Health Sciences, Fred Hutchinson Cancer Research Center, 1100 Fairview Ave N, Seattle, WA, 98109

[4]Department of Biochemistry, University of Washington, Seattle WA 98195

[5]Department of Ophthalmology, University of Washington, Seattle WA 98195

[6]Department of Oncological Sciences, Huntsman Cancer Institute, University of Utah, 2000 Circle of Hope, Salt Lake City, UT 84112

SUMMARY

Deregulated Myc transcriptionally reprograms cell metabolism to promote neoplasia. Here we show that oncogenic Myc requires the Myc superfamily member MondoA, a nutrient-sensing transcription factor, for tumorigenesis. Knockdown of MondoA, or its dimerization partner Mlx, blocks Myc-induced reprogramming of multiple metabolic pathways resulting in apoptosis. Identification, and knockdown, of genes co-regulated by Myc and MondoA has allowed us to define metabolic functions required by deregulated Myc and demonstrate a critical role for lipid biosynthesis in survival of Myc-driven cancer. Furthermore, overexpression of a subset of Myc and MondoA co-regulated genes correlates with poor outcome of patients with diverse cancers. Co-regulation of cancer metabolism by Myc and MondoA provides the potential for therapeutics aimed at inhibiting MondoA and its target genes.

*Correspondence: eisenman@fhcrc.org.
#Co-First Author

INTRODUCTION

The *MYC* proto-oncogene family includes *MYC* that encodes c-Myc, *MYCN* that encodes N-Myc, and *MYCL* that encodes L-Myc. Myc proteins are bHLHZ transcription factors that regulate genes involved in growth and proliferation (Dang, 2012). *MYC* genes are normally induced in response to mitogenic stimulation. However oncogenic activation occurs through events that lead to overexpression of Myc proteins and failure to downregulate expression in response to appropriate physiological signals.

Deregulated Myc family proteins transcriptionally reprogram cellular metabolism to facilitate the macromolecular synthesis required for increased cell growth and proliferation. For example, c-Myc induces aerobic glycolysis (the Warburg effect) by enhancing glucose uptake and lactate production as well as providing glycolytic intermediates for nucleotide, amino acid and lipid biosynthesis (reviewed in Dang, 2013; Vander Heiden et al., 2009). While these processes divert carbon from the TCA cycle and mitochondria, c-Myc also regulates genes that enhance glutamine uptake and processing in order to fuel the TCA cycle (Gao et al., 2009; Wise et al., 2008; Yuneva et al., 2007), moreover c-Myc stimulates mitochondrial activity through induction of *TFAM* and other nuclear-encoded mitochondrial genes (Li et al., 2005). Recent work demonstrates that c-Myc promotes lipid metabolism during cell cycle entry (Morrish et al., 2010) and lymphomagenesis (Eberlin et al., 2014). Importantly, cells transformed by deregulated *MYC* genes are highly sensitive to metabolic stress induced by nutrient withdrawal or inhibition of metabolic pathways (reviewed in Dang, 2011).

Myc proteins function within a transcription factor network (Figure 1A)(Conacci-Sorrell et al., 2014). These proteins form heterodimers with the small bHLHZ protein Max, which bind to E-Box sequences in DNA. Myc transcriptional activity is antagonized by Mxd family proteins that compete with Myc for both Max and E-Box binding. Expression of Mxd proteins often correlates with cell cycle exit, growth arrest and/or differentiation (Hooker and Hurlin, 2006). In addition, a parallel, Myc-like network exists centered around Mlx (Billin and Ayer, 2006). Mlx heterodimerizes with either MondoA or carbohydrate response element binding protein (ChREBP). MondoA associates with the mitochondrial outer membrane, where it can sense both glycolytic intermediates such as glucose 6-phosphate and mitochondrial metabolites (Han and Ayer, 2013; Kaadige et al., 2009; Sloan and Ayer, 2010). Metabolites promote nuclear localization of cytoplasmic MondoA protein, activating transcription of genes involved in glucose metabolism. (reviewed in O'Shea and Ayer, 2013). Moreover, Mlx heterodimerizes with a subset of Mxd family proteins, thereby linking the Mlx and Max branches into a larger transcription factor network (Figure 1A)(Billin et al., 1999; Meroni et al., 2000). This network is conserved throughout metazoan evolution (McFerrin and Atchley, 2011), indicative of collaboration between the nutrient-sensing Mondo and the nutrient-utilizing Myc branches of the network.

Because environmental context can determine survival of cells transformed by Myc family proteins, we reasoned that the extended Myc-network is likely to be important in integrating environmental cues and promoting tumor survival.

RESULTS

Synthetic lethal interaction between deregulated Myc and MondoA loss of function

To determine whether deregulated Myc is dependent on other transcription factors within the Myc superfamily, we carried out a targeted siRNA screen of the extended Myc network. The screen employed murine fibroblasts with doxycycline (dox)-inducible c-Myc expression (clone P3C1). Induction of c-Myc (c-Myc-ON) resulted in increased proliferation and apoptosis as well as loss of the differentiation marker Thy1.2 (Eischen et al., 2001; Evan et al., 1992; Sridharan et al., 2009)(Figures S1A–C). Our most striking finding was that knockdown of MondoA and, to a lesser extent, its obligate dimerization partner Mlx, revealed a synthetic lethal (SL) effect in c-Myc-ON compared to c-Myc-OFF cells (Figures 1B and S1D). Knockdown of ChREBP had no effect since it is not expressed in P3C1 cells (Figure S1E).

To extend our observations on the dependency of Myc overexpressing cells on MondoA/Mlx we examined mouse embryonic fibroblasts (MEFs) bearing homozygous deletions of either *Mlxip*, which encodes MondoA, or *Mlx* (unpublished data). Compared to the parental wild-type cells, both *Mlxip*$^{-/-}$ and *Mlx*$^{-/-}$ primary MEFs display reduced viability and higher levels of apoptosis upon c-Myc overexpression. *Mlxip* deletion also enhances c-Myc mediated apoptosis in Large-T antigen immortalized fibroblasts, suggesting a p53-independent apoptotic process (Figure S1F and see below).

We next examined the effects of MondoA knockdown (KD) in a panel of human cell types, in each case comparing cells without and with overexpression of Myc. We found that KD of MondoA using siRNA (siMonA) significantly reduces survival of the P493-6 human B cell line expressing c-Myc (Figure 1C and S1G). This synthetic lethal (SL) effect was also observed with siMonA in human neural stem cells (CB660) overexpressing c-Myc (CB660+c-Myc) as well as their immortalized derivatives lacking p53 and RB tumor suppressors (I-CB660+c-Myc) or transformed by the additional expression of activated H-Ras (T-CB660+c-Myc) (Hubert et al., 2013) (Figure 1D). Control cells were insensitive to siMonA, indicating that MondoA loss of function specifically inhibits survival of cells with deregulated c-Myc. MondoA silencing also inhibits the growth of colon cancer cell line HCT116, hepatocellular carcinoma cell line HEPG2, and ovarian cancer cell line TOV1112D, all of which express high levels of c-Myc (Figure S1H). Importantly, siRNA against Mlx also elicited the same response in all cells tested (data not shown).

MYCN amplification is observed in approximately 25% of human neuroblastomas (NB) and correlates with poor outcome (Brodeur, 2003; Huang and Weiss, 2013). Therefore, we examined the requirement of deregulated N-Myc for MondoA, using a retroviral vector to achieve stable MondoA KD (Kaadige et al., 2009) in human NB cell lines. Upon MondoA silencing, *MYCN* amplified IMR32 and SK-N-BE cells and Tet21N cells overexpressing N-Myc displayed reduced viability compared to the *MYCN* non-amplified SH-SY-5Y or the Tet21N cells in which N-Myc is not overexpressed (Figure 1E). Reduction of MondoA protein levels following knockdown is shown in Figure S1I. We did not detect changes in Myc protein levels after MondoA silencing, indicating that loss of MondoA does not inhibit cell proliferation by reducing Myc expression (See below in Figure S2A,H,I,J). However, c-

Myc or N-Myc induction enhances MondoA mRNA (Figures S1J,K) and protein levels in both cytoplasm and nucleus (Figure 1F and S1L) in Tet21N and P493-6 cells. This is consistent with our chromatin immunoprecipitation data for N-Myc (Figure S1M), as well as data from the ENCODE database (not shown), showing that c-Myc binds the MondoA promoter region.

Because MondoA would be expected to compete with several Mxd transcription factors for binding to Mlx, we surveyed expression levels of Mxd1, Mxd4 and Mnt upon N-Myc activation in Tet21N cells. N-Myc overexpression reduces c-Myc and Mxd4 protein expression while increasing Max, Mlx and MondoA proteins (Figure S1N). Consistent with this, the expression of the MondoA target gene Txnip increases upon N-Myc activation (Figure S1O). Our experiments suggest that deregulated Myc alters the Max/Mlx network to enhance MondoA/Mlx transcriptional activity and moreover requires MondoA/Mlx for survival and proliferation.

MondoA suppresses Myc-induced apoptosis in neuroblastoma

To study functional interactions between N-Myc and MondoA we used the Tet21N cell line (Lutz et al., 1996). Tet21N cells in the presence of dox (N-Myc-OFF) express endogenous c-Myc and proliferate but are non-tumorigenic. Following dox withdrawal, N-Myc is induced (N-Myc-ON) in Tet21N cells and cells display increased proliferation and growth in soft-agar and as xenografts (Kim et al., 2007; Wasylishen et al., 2013). We assessed proliferation, cell cycle and apoptosis in Tet21N cells under four conditions: siCtrl or siMonA with and without dox. Transient siMonA blocked proliferation of the Tet21N N-Myc-ON cells, while having little or no effect on the N-Myc-OFF cells, compared to siCtrl (Figure 2A). Each of the four individual siRNAs efficiently silences the expression of MondoA and only inhibits the growth of N-Myc-ON cells, indicating the phenotype we observed is a result of MondoA inactivation (Figure S2A). While siMonA marginally reduces the percentage of cells in S phase independent of N-Myc levels, there is a striking accumulation of sub-G1 cells in the siMonA N-Myc-ON cells, indicative of apoptosis (Figure 2B,C). MondoA KD also blocked expression of its target gene *TXNIP* (Figures 2D and S2B)(Stoltzman et al., 2008), and suppressed mTOR activity (Figure 2D). We also detected increased levels of p53 and p21 with siMonA, which are further increased after N-Myc activation (Figure 2D). Our data suggest MondoA suppresses stress associated with N-Myc deregulation and ensures cell cycle progression and survival.

The tumorigenic potential of Tet21N cells stably expressing either shCtrl or shMonA was first assessed by soft-agar assays. While shCtrl N-Myc-ON cells form numerous colonies, shMonA N-Myc-ON cells formed fewer and smaller colonies (Figures 2E,F). MondoA silencing also reduced the growth of N-Myc amplified cell lines in soft agar (Figure 2F). Importantly, the diminished cloning efficiency in shMonA N-Myc-ON cells and reduced viability of HCT116 cells expressing shMonA were rescued by the expression of an shRNA-resistant MondoA (Figure 2F, S2C,D). Finally, ectopic expression of MondoA in knockdown cells suppresses N-Myc mediated activation of p53 and p21 (Figure S2E), and restores expression of the MondoA target gene *TXNIP* (Figure S2F), ruling out off-target effects of either shRNA or siRNA.

We also performed subcutaneous xenograft of Tet21N N-Myc-ON cells stably expressing either shCtrl or shMonA. We observed reduced tumor size and tumor weight of cells expressing shMonA (Figure 2G, 2H) due to both loss of proliferation and activation of apoptosis (Figures 2I and S2G). Both N-Myc protein stability in the Tet21N cells (Figure S2H) and abundance in lysates derived from the xenografts (Figure S2I) are independent of MondoA. Very similar SL interactions were obtained in the P493-6 human lymphoma line. (Figures 1C and S2J). We conclude that MondoA is broadly required for downstream functions of Myc in tumor growth and survival in vitro and in vivo.

N-Myc and MondoA coordinately regulate expression of growth promoting genes

To ask if MondoA loss affects N-Myc functions we compared transcriptional changes induced by N-Myc activation in the presence or absence of MondoA (Figures 3A and S3A,B,C). Overall, the N-Myc induced changes in gene expression are highly correlated independent of MondoA levels (Figure S3B). Moreover, MondoA knockdown does not alter the levels of histone H4 acetylation observed upon N-Myc induction (Figure S3D), indicating MondoA functions in conjunction with Myc, but does not fundamentally alter N-Myc activity.

However, while the general transcriptional activity of N-Myc is similar in the presence or absence of MondoA, the magnitude of change for both N-Myc activated and repressed genes is significantly attenuated in the siMonA condition compared to siCtrl (Figure 3B). Interestingly, after normalizing gene expression values to the siMonA/N-Myc-OFF condition and comparing the relative contributions of N-Myc and MondoA alone, we observe a trend in which both transcription factors similarly up- or down-regulate a large number of genes in common (Figure S3E). Specifically, we identified 553 and 587 genes significantly upregulated and downregulated, respectively, when both N-Myc and MondoA are present (Figure 3A,C)

To assess the functional relevance of these transcriptional profiles, we used Gene Ontology analysis of the gene sets individually and cooperatively regulated by N-Myc and MondoA (FDR adjusted p value<0.05). N-Myc primarily drives the expression of genes promoting cell proliferation and growth (Figure 3D, white bars). However, N-Myc also requires MondoA to maximally upregulate a large number of genes involved in these processes (Figure 3D, striped bars). The relative expression levels of all cooperatively upregulated genes among the four conditions are shown in Figure 3E. Interestingly, among these are several genes critical for nucleotide biosynthesis, amino acid metabolism and transport, mitochondrial biogenesis and function, and the TCA.

We also find that silencing of MondoA independent of N-Myc leads to lower expression of genes involved in oxidation-reduction reactions, cholesterol and steroid metabolism, as well as components of the endoplasmic reticulum, extracellular matrix, peroxisomes, and lysosomes (Figure 3F, grey bars). In particular, MondoA depletion leads to a strong decrease in *SREBP1* and *SCD* expression, as well as a lesser reduction in the *FASN* and *PCK2*, which encode enzymes involved in lipid and glucose metabolism, respectively (Figure 3G). Hence, N-Myc, individually and in cooperation with MondoA, controls the expression of a large set

of genes involved in proliferation, metabolism and growth, while MondoA additionally regulates complementary pathways such as lipid and sterol biogenesis.

There may be several mechanisms for the cooperative transcriptional regulation by N-Myc and MondoA. To determine whether both factors co-occupy promoters of coregulated genes we tested if N-Myc and MondoA bind to the *TXNIP* promoter, a bona fide MondoA target that contains three non-canonical E-boxes. Results show that both factors bind to the *TXNIP* promoter and that maximum binding of both N-Myc and MondoA requires the simultaneous presence of both factors (Figure S3F and Discussion).

Expression of Myc/MondoA dependent genes involved in metabolism is required for survival of neuroblastoma cells

Our data show that a significant fraction of genes regulated by N-Myc and MondoA are linked to metabolic activities (Figures 3D–G). We utilized qRT-PCR and immunoblot analyses to assess expression of a subset of genes under the four conditions employed in the microarray study, focused on those impacting multiple metabolic pathways, and found that all genes analyzed require either N-Myc/MondoA or MondoA for maximal expression (Figures 4A and S4A). The expression of these genes were similarly affected by silencing of the MondoA heterodimerization partner Mlx in Tet21N cells, consistent with the notion that changes in expression we observed are a direct consequence of the lack of MondoA-Mlx heterodimers (Figure S4B). Interestingly, silencing of either MondoA or Mlx results in the loss of expression of both proteins, indicating that heterodimerization promotes complex stability (Figure S4B).

Because we also observe synthetic lethality in P493-6 B cells, we queried oncomine.org for datasets of B cell malignancies (Basso et al., 2005; Zhang et al., 2013). We found a correlation between c-Myc, Mlx (in one dataset) and many target genes in both Burkitt's Lymphoma and other B cell malignancies as well as neuroblastoma (Table S1) (Janoueix-Lerosey et al., 2008; Wang et al., 2006), consistent with the notion of similar transcriptional reprogramming of metabolism by the coordinate action of Myc-Max and MondoA-Mlx arms of the network. Using MondoA or Mlx null primary MEFs we found expression of Slc1A5 and Tomm20, both of which are coregulated in the Tet21N cells, to be dependent on both Myc and MondoA (Figure S4C), implying that c-Myc and MondoA display a similar mode of co-regulation in primary cells.

We also confirmed that N-Myc requires both 25 mM glucose and MondoA to fully activate the expression of the glutamine (Gln) transporter Slc1A5, suggesting that glucose-responsive transcriptional activity of MondoA coordinates glucose availability with Gln uptake (Figure 4B). To determine whether cellular metabolism is affected by MondoA knockdown in the Tet21N cells, we measured carbon source uptake using radiolabeled Gln or 2-deoxyglucose (2DG). A notable increase in Gln uptake was observed upon N-Myc activation, which was inhibited by shMonA treatment in both the N-Myc-ON Tet21N cells (Figure 4C) and in c-Myc overexpressing MEFs (Figure S4D). Consistent with the glucose dependency of Slc1A5 expression, maximal N-Myc-induced Gln uptake was also glucose-dependent (Figure S4E). By contrast, N-Myc expression or MondoA knockdown produced only a modest increase in 2DG uptake and no significant difference was observed between

control and SL conditions (Figure S4F). Furthermore, while extracellular acidification rate was not significantly affected by N-Myc expression or shMonA (Figure S4G), MondoA loss prevented the N-Myc driven increase in Gln-dependent oxygen consumption rate (Figure 4D), confirming that MondoA loss in cells expressing N-Myc results in fundamental changes in cellular Gln metabolism.

Decreased expression of transporter genes may account, at least in part, for diminished Gln uptake and viability upon MondoA loss (Figures 4A and S4A). As previously shown, knockdowns of either Gln importer Slc1A5 or anti-transporter Slc3A2 resulted in decreased activity of mTOR, as measured by ribosomal protein S6 phosphorylation (p-RpS6) (Figure 4E) (Duran et al., 2012; Nicklin et al., 2009). However, only Slc1A5 silencing reduced Gln uptake, arguing that loss of Slc3A2 does not affect cell viability and mTOR signaling by preventing Gln uptake (Figure S4H). Importantly, while overexpression of Slc1A5 enhances Gln uptake (Figure S4I), neither Slc1A5 nor Slc3A2 overexpression rescues cell viability (Figure 4F). Therefore, reduced Gln uptake is not solely responsible for the observed SL phenotype.

Loss of MondoA attenuates the expression of genes involved in other metabolic pathways; therefore we asked how the individual KD of co-regulated or MondoA-dependent genes influences Tet21N cell survival. As shown in Figure 4G, siRNAs against 15 out of 21 selected targets were significantly more efficient at killing cells overexpressing N-Myc. Depletion of a subset of these targets in CB660 human NSCs confirmed that the single gene KD phenotype is Myc-specific in different cell lines (Figure S4J).

Inhibition of Myc/MondoA dependent genes induces p53-independent synthetic lethality with deregulated Myc

Because the activity of mTOR and p53 are often inversely correlated under stress conditions (Feng and Levine, 2010), we evaluated whether the individual silencing of other Myc SL metabolic genes affects p-RpS6 and p21 levels, as indicators of mTOR and p53 activity, respectively. While only inactivation of Pfas, Cbs or Pck2 results in mTOR inhibition, all knockdowns induce p21 to varying levels (Figure 5A). This suggests that p53 senses the activity of multiple Myc- and MondoA-regulated pathways.

To evaluate the response of Tet21N cells to p53 activation, we used the MDM2 antagonist Nutlin-3a, which strongly induces both p53 and p21 and inhibits growth of both N-Myc-OFF and -ON cells (Figure 5B,C). However, Nutlin-3a treatment does not stimulate significant caspase activity in siCtrl cells, regardless of N-Myc status (Figure 5C), indicating that p53 activation promotes cell cycle arrest but not apoptosis in these cells. Conversely, loss of MondoA alone promotes caspase activity in N-Myc-ON cells, which is further enhanced by Nutlin-3a treatment (Figure 5C). This implies that MondoA silencing in N-Myc-ON cells induces apoptosis, and that p53 activation only contributes to apoptosis following loss of MondoA. Importantly, we observe caspase activation only when N-Myc is overexpressed. Furthermore, complete knockdown of p53 in the N-Myc-ON cells only partially rescues viability with siMonA (Figure 5D). Moreover, while p53 KD re-establishes RpS6 phosphorylation, it does not reestablish expression of Myc and MondoA target genes Pfas and Tomm20, indicating that the reduction in mTOR activity is a consequence of

apoptosis and not the cause of the SL phenotype (Figure S5A). Moreover, HCT116 cells (Figure 5E and S5B), or CB660 cells (Figure S4J) and MEFs overexpressing c-Myc (Figure S5C) are equally sensitive to loss of MondoA, Mlx, or a number of critical Myc/MondoA targets, independent of p53 status. In addition, siMonA also results in the loss of Slc1A5, Pfas and Tomm20 expression and decreased Gln uptake independent of p53 in HCT116 cells (Figure S5D,E) confirming that MondoA loss promotes apoptosis, at least in part, through a p53-independent mechanism.

We also find that loss of MondoA (Figure 5F) or Mlx (Figure S5F) leads to downregulation of the pro-survival Bcl2 protein and promotes the appearance of the proapoptotic, truncated forms of Bid and Bax (tBid and tBax) and cleaved Parp, only in N-Myc-ON cells. These data indicate that N-Myc overexpression is required to promote apoptosis in the absence of MondoA through an intrinsic apoptotic pathway. However, enforced expression of Bcl2 was not sufficient to rescue viability in N-Myc-ON, siMonA cells (Figure 5G). These results prompted us to search for alternative MondoA-dependent metabolic pathways required for N-Myc induced tumorigenesis.

Metabolic profiling reveals that N-Myc and MondoA coordinately regulate anaplerotic and cataplerotic reactions of the tricarboxylic acid cycle

We utilized LC-MS based metabolomic analysis to survey 139 soluble metabolites representing precursors and intermediates of major anabolic and catabolic pathways (see Supplemental Experimental Procedures). As shown in Figure 6A, we detect significant changes in metabolite abundance amongst the four conditions. Metabolite set enrichment analysis (MSEA) reveals that N-Myc activation broadly modifies the cellular metabolic profile, promotes profound changes in amino acid metabolism and results in enhanced abundance of precursors for de novo purine and lipid biosynthesis (Figure 6B; blue bars). Importantly, the majority of MSEA categories enriched by N-Myc induction display diminished significance upon siMonA treatment in our SL condition (Figure 6B, orange bars). Consistent with the observed cooperative transcriptional regulation of metabolic genes, we observe that maximal enrichment of certain metabolites, such as the nucleotide sugar Ribose-5-Phosphate (R5P) and the isoprenoid geranyl-pyrophosphate (GPP) is dependent upon both N-Myc and MondoA. We also observe diminished levels of glutamate (Glu) and malate (Mal) and a five–fold increase in citrate (Cit) upon MondoA silencing (Figure S6A and data not shown). These data indicate alterations in the TCA cycle as a result of mitochondrial dysfunction, consistent with our observations of diminished mitochondrial content and activity, and enhanced ROS production (Figure S6B,C).

Because we observed diminished Gln uptake and alterations in abundance of TCA cycle intermediates, we directly tested how Gln metabolism is modified by N-Myc and MondoA. We employed a GC-MS method (Du et al., 2013) to trace the contribution of uniformly labeled $^{13}C_5$-Gln to Glu, α–ketoglutarate (αKG), Mal, Cit, pyruvate (Pyr) and lactate (Lac). We chose 24 hr labeling in order to account for metabolites upstream and downstream of the TCA. Figure 6C shows that loss of MondoA results in a decreased N-Myc dependent fractional contribution of $^{13}C_5$-Gln to metabolite pools downstream of the glutaminase reaction, as indicated by decreased metabolism of Gln (mass of glutamine + 5(^{13}C) = m+5)

to Glu (m+5), αKG (m+5), Mal (m+4) but, paradoxically not TCA derived Cit (m+4). We did not detect $^{13}C_5$-Gln contributing to either Pyr or Lac (data not shown) indicating that Gln is filling the TCA and not being converted to Pyr, via cytosolic malic enzyme, then, via Ldha, to Lac.

To directly test if reduced glutaminolysis and mitochondrial activity are responsible for the synthetic lethal phenotype, we evaluated the response of Tet21N cells to both nutrient withdrawal and metabolic perturbing agents (Table S2). These cells are both glucose and Gln-dependent, sensitive to common glutaminolysis perturbing agents, such as the non-specific transaminase inhibitor aminooxyacetate (AOA)(Szabo et al., 2013; Wise et al., 2008), the OXPHOS complex I inhibitor metformin (MET), or the Pck1/Pck2 inhibitor 3-mercaptopicolinic acid (3MP), and sensitive to oxidative stress induced by H_2O_2. We also tested pathway-specific metabolites for their ability to rescue loss of viability induced by treatment with inhibitors or siMonA. While none of the rescue agents can substitute for glucose or Gln, each specific inhibitor can be rescued by metabolites downstream of the inhibited pathway. Similar sensitivities to these inhibitors were observed in HCT116 cells, independent of p53 status (Table S2 and data not shown).

Importantly, none of the agents used to rescue impaired glutaminolysis, such as dmKG, Pyr or enforced Slc1A5 or Bcl2 expression (Wise et al., 2008; Yuneva et al., 2007) is sufficient to rescue loss of MondoA (Table S2 and data not shown). Therefore, we ruled out a solely anaplerotic defect, and interrogated pathways downstream of the TCA. As noted, Cit accumulates by 6-fold in the SL condition, as confirmed by GC-MS of total Cit (Figure 6D). Because Cit is produced from αKG either through the TCA cycle (producing m+4 Cit) or via IDH mediated reductive carboxylation (producing m+5 Cit) (Figure S6D) we quantified m+5 Cit by GC-MS. We find a dramatic reduction in the m+5 Cit fraction under the SL condition (Figure S6E), indicating that, while the fate of Gln-derived αKG is modified under our four conditions, the increased Cit content is not due to enhanced synthesis. Thus the marked accumulation of Cit could result from its diminished downstream utilization for de novo fatty acid or isoprenoid biosynthesis. Consistent with this hypothesis, we observed that loss of MondoA results in the downregulation of Srebp1, Fasn and Scd, (Figure 4A) all of which participate in the lipid biosynthesis pathway. Because Cit can be converted to acetyl-coA for de novo fatty acid synthesis (Figure S6D) we tested if Gln-derived carbons contribute to lipid and if loss of MondoA impairs lipid biosynthesis. To this end, we employed a lipid extraction protocol and GC-MS (Metallo et al., 2012) for tracing Gln-derived carbons to palmitate (C16:0) in the free fatty acid pool, 48 hr after the addition of $^{13}C_5$-Gln. While N-Myc cooperates with MondoA to provide Gln as anaplerotic substrate to generate Cit, MondoA is further required to convert Cit into fatty acids, as the total fraction of labeled palmitate (sum of m+2(N) palmitate) drops from about 20% to less than 15% of the pool, upon MondoA silencing, independent of N-Myc (Figures 6E and S6F). Consistent with loss of Fasn expression the fraction of labeled palmitate (m+4 to m+12) is significantly diminished (Figure 6E).

Deletion of *Mlx* in MEFs expressing endogenous Myc also leads to decreased expression of MondoA, Fasn, and other targets and reduced lipid content, but does not induce apoptosis (Figure S6G–J, and data not shown) Therefore diminished de novo fatty acid biosynthesis

observed in the synthetic lethal condition is not a consequence of apoptosis but the metabolic response to the loss of MondoA-Mlx transcriptional activity and target gene expression.

To confirm the dependency of N-Myc overexpressing cells on lipid biosynthesis for viability we tested the sensitivity of Tet21N cells to the Fasn inhibitor C75 and the farnesyl diphosphate synthase (Fdps) inhibitor zoledronic acid (ZOL), which blocks GPP production. Consistent with the siRNA results, N-Myc overexpressing cells are significantly more sensitive to these inhibitors and there is no effect on viability of N-Myc-OFF cells when treated with the IC50 of N-Myc-ON cells (Figure S6K). Furthermore, C75, but not ZOL treatment synergizes with siMonA to hyperactivate caspase (Figure 6F, and S6L), suggesting a sensitization to loss of FASN activity and consistent with decreased flux into palmitate. Similarly, siRNA mediated silencing of Fasn or Scd enhances apoptosis in N-Myc-ON cells (Figure S6M). In addition, while the effect of ZOL treatment can be rescued by the downstream metabolite geranylgeraniol (GGOH)(Table S2), this metabolite fails to rescue loss of viability in siMonA N-Myc-ON cells, indicating that inhibition of the isoprenoid pathway is not the causal event of our SL phenotype. Because C75 treatment can be rescued by oleate (C18:1) (Table S2), we tested if oleate can rescue viability of siMonA N-Myc-ON cells. As shown in Figures 6G,H and S6N, oleate suppresses activation of stress upon siMonA treatment and partially restores cell viability, thus placing the failure of lipid biosynthesis upstream of the cascade of stress-inducing events leading to the SL phenotype.

A subset of synthetic lethal genes correlates with poor outcome in several cancers

Our data indicate that Myc and MondoA coordinately and independently enhance the expression of multiple metabolic genes to promote tumorigenesis (Figure 7A). If so, high expression of several of these genes in human cancers would be predicted to correlate with poor prognosis. Using the cumulative expression of *MLXIP*, *CAD*, *TFAM*, *CBS*, *SCD*, *PFAS*, *SLC3A2*, and *SLC1A5*, we calculated the overall survival of patients with different types of cancer and found that, in most cases, patients with high expression of the signature (top 20%, red) have poorer prognosis compared to those with low expression (bottom 20%, blue; the remaining 60% are shown in grey) (Figures 7B). However, while the difference between high and low expressing patients is significant in Neuroblastoma, LIHC and LUNG, it is only marginally significant in LAML and COAD and not significant in BRCA. This reflects the inherent heterogeneity of cancer and it is consistent with a recent report demonstrating that c-Myc overexpression elicits distinct metabolic programs in different tissues (Yuneva et al., 2012).

DISCUSSION

Proliferation and metabolism are precisely coordinated processes during normal cell growth and division and are frequently deregulated in cancer. A unique property of the Max/Mlx network is its capacity to sense and respond both to mitogenic signals and nutrient availability (Diolaiti et al., 2014; O'Shea and Ayer, 2013). In this study we provide evidence that the MondoA-Mlx heterodimer is required for Myc-driven transcriptional reprogramming of cellular metabolism and tumor growth. We show that MondoA/Mlx

coordinates glucose-sensing with Gln utilization and subsequent downstream biosynthesis required for Myc to promote hyperproliferation. Previous work has demonstrated a critical role for Gln in survival of Myc driven cancers (Dang, 2011; Qing et al., 2012; Shachaf et al., 2007; Wise et al., 2008; Yuneva et al., 2007). Here we show that MondoA loss suppresses Myc-induced GLN uptake, GLN-dependent mitochondrial activity and Gln-derived lipid biosynthesis, thus resulting in apoptosis. In support of our findings, MondoA was reported to be overexpressed in acute lymphoblastic leukemia (ALL), and its silencing prevents tumor cell growth (Wernicke et al., 2012). The SL phenotype described here places MondoA atop a transcriptional cascade that coordinately regulates multiple metabolic pathways critical for Myc-driven tumor survival.

Impairment of Myc/MondoA downstream metabolic effectors identified in this study has permitted us to define SL interactions specific to deregulated Myc. These include those involved in glucose, amino acid, nucleotide, mitochondrial function, and lipid metabolism. While Myc's connection with, and dependency upon, enhanced glycolysis, glutaminolysis and mitochondrial activity are well known, a role for Pck2, a gluconeogenic enzyme, reveals a requirement of Myc for a bidirectional pathway. Recent reports demonstrating the necessity for Pck2 activity in both lung and breast cancer cells under nutrient limitation (Leithner et al., 2014; Mendez-Lucas et al., 2014) are consistent with MondoA-Mlx function as a nutrient-responsive factor to regulate survival.

We also observed impairment of lipid metabolism in our SL condition. While the MondoA family member ChREBP has been linked to glucose-derived lipogenesis in cancer cells (Tong et al., 2009), ChREBP has not been reported to alter glutaminolysis and its requirement for Myc driven tumorigenesis remains untested. Our data supports non-redundant roles for MondoA and ChREBP, as siRNA against MondoA (as well against Mlx) kills ChREBP-expressing cells.

Multiple studies have shown that inhibition of Acaca, Fasn or Scd activity (Zaidi et al., 2013) as well as loss of Srebp1 (Griffiths et al., 2013) attenuates cancer cell growth. Interestingly, we find that oleate partially rescues these insults as well as apoptosis due to MondoA suppression in cells with high Myc levels. Our study reveals the importance of lipogenesis in Myc-dependent metabolic reprogramming and provides a rationale for the clinical evaluation of lipogenesis inhibitors in Myc-driven malignancies. This is highly relevant in light of the recent report of altered lipidomic profiles induced by Myc in human lymphomas (Eberlin et al., 2014)

Importantly, in contrast to all other Myc network members, Mondo proteins are ligand activated, as they sense glucose-6-phospate (G6P) and other glycolytic intermediates (McFerrin and Atchley, 2012; Peterson et al., 2010; Stoltzman et al., 2008). Blocking the ability of MondoA to respond to glucose may represent a therapeutic strategy targeting Myc-driven tumors. In addition, a small molecule inhibitor of c-Myc-Max heterodimerization has been described (Wang et al., 2007), indicating the feasibility of developing inhibitors of Mondo-Mlx heterodimerization.

Previous studies have clearly established functional antagonism between Myc and Mxd/Mnt proteins in the control of cell behavior (Hooker and Hurlin, 2006). However, recent work demonstrating a role for Mnt in Myc-driven tumor progression (Link et al., 2012), in conjunction with our report describing Myc-MondoA transcriptional synergy, suggests a more complex scenario in which an imbalance among network members promotes apoptosis.

How do N-Myc and MondoA cooperate to promote the transcription of their metabolic gene targets? One possibility involves simultaneous binding of both N-Myc and MondoA to promoters containing multiple E-boxes for maximal gene expression. Binding of c-Myc and either MondoA or ChREBP to the *LDHA* and *HKII* (Sans et al., 2006) or *PKLR* (Zhang et al., 2010) promoters has been described and we demonstrate that both N-Myc and MondoA bind to the *TXNIP* promoter. We also show that, N-Myc activation promotes Mondo-Mlx activity by altering the expression of MondoA and other network members competing for the common heterodimerization partner Mlx. Conversely, loss of MondoA may inhibit N-Myc transcriptional activity by altering chromatin at metabolic target gene promoters to abrogate N-Myc transcriptional amplification (Lin et al., 2012; Nie et al., 2012). Moreover, in the absence of MondoA, the Mxd and Mnt proteins may heterodimerize with Mlx and actively repress N-Myc/MondoA target genes. These mechanisms are not mutually exclusive and may operate in a cell type and promoter-specific manner.

Although much attention has been focused on Myc because of its oncogenic activity, we propose that a full understanding of Myc biology in both physiological and pathological contexts will require an understanding of the biology and dynamics of the Max/Mlx network as a whole.

EXPERIMENTAL PROCEDURES

A complete list of all techniques and reagents, such as enzyme inhibitors, retroviral, and lentiviral vectors and in vitro functional assay are listed in the Supplementary Experimental Procedures.

Xenograft

1×10^6 Tet21N cells were resuspended in *Growth Factor Reduced (GFR), Phenol Red-free BD Matrigel*™ (Becton Dickinson) and subcutaneously injected into the flanks of nude athymic (nu/nu) mice (n=10). Tumor volume was measured every 2–3 days and mice were sacrificed when tumor burden reached a total volume of 2.5 cm^3. Tumors were dissected and aliquots were either frozen in liquid nitrogen or fixed in formalin for further analysis. Immunistochemistry analysis was performed in the Fred Hutchinson Cancer Research Center Experimental Histopathology Core. The Fred Hutchinson Cancer Research Center Institutional Animal Care and Use Committee approved all mouse experiments.

Gene Expression Analysis

Whole genome expression analysis was performed using Illumina HumanHT-12 v4 Expression BeadChip. Sample processing was performed at the Fred Hutchinson Cancer Research Center Genomics Facility and data was submitted to Gene Expression Omnibus

(Accession Number of dataset in GEO: GSE55538). For details about data statistical analysis see below.

Metabolomic Profiling

Cell processing: 48 hr after transfection 1×10^6 cells were plated in a 6 well plate. After 24 hr culture media was aspirated, cells were washed twice in ice cold H_2O and lysed in 1.5 mL of ice cold 9:1 methanol:chloroform with the plates placed on dry ice (~−75°C) to quench metabolism. After 5 minutes, cells were scraped and transferred into 1.5 ml tubes. Lysates were centrifuged at 13000 RPM for 10 min and supernatants were transferred to new vials and dried using a Speedvac at room temperature. After reconstituting the dried samples in water and 1% formic acid, they were subjected to LC-MS analysis (see Supplementary Experimental Procedures). Metabolite levels were normalized to cell number from parallel plates. For details about data statistical analysis see below.

Statistical Analysis

Statistical significance of all in vitro experiments was calculated by using Graphpad Prism software with either a Student's T test for comparisons of only 2 conditions, or ANOVA and a Bonferroni Correction for multiple comparisons. Gene expression data were run in triplicate with quantile normalized and log transformed values. Significance was determined by Benjamin Hotchberg (BH) FDR adjusted p-value< 0.05 according to the lumi package using R version 3.0.1 (Du et al., 2008). Gene Ontology enrichment was reported for categories satisfying BH adjusted p-value < 0.05 from DAVID boinformatic database (Huang da et al., 2009). Metabolite data were normalized to the N-Myc OFF and siCtrl condition with log-transformed z-scores. Metabolite pathway enrichment was performed using Metaboanalyst (Xia et al., 2012) with metabolite sets having FDR corrected p-value<0.05 deemed significant. Both gene and metabolite heatmaps show median z-scores of each triplicate sample using Cluster and TreeView (Eisen et al., 1998).

Kaplan-Meier Survival Curves

Kaplan Meier curves were calculated for gene expression data obtained for Neuroblastoma (Oberthuer et al., 2006) as well as BRCA, LUNG, COAD, LAML, and LIHC reported by The Cancer Genome Browser (Lopez-Bigas N et al., 2013) for The Cancer Genome Atlas (TCGA) (additional details in Supplemental Experimental Procedures).

Supplementary Material

Refer to Web version on PubMed Central for supplementary material.

Acknowledgments

References

Basso K, Margolin AA, Stolovitzky G, Klein U, Dalla-Favera R, Califano A. Reverse engineering of regulatory networks in human B cells. Nat Genet. 2005; 37:382–390. [PubMed: 15778709]

Billin AN, Ayer DE. The Mlx network: evidence for a parallel Max-like transcriptional network that regulates energy metabolism. Curr Top Microbiol Immunol. 2006; 302:255–278. [PubMed: 16620032]

Billin AN, Eilers AL, Queva C, Ayer DE. Mlx, a novel Max-like BHLHZip protein that interacts with the Max network of transcription factors. J Biol Chem. 1999; 274:36344–36350. [PubMed: 10593926]

Brodeur GM. Neuroblastoma: biological insights into a clinical enigma. Nat Rev Cancer. 2003; 3:203–216. [PubMed: 12612655]

Conacci-Sorrell M, McFerrin L, Eisenman RN. An Overview of MYC and Its Interactome. Cold Spring Harb Perspect Med. 2014; 4:a014357. [PubMed: 24384812]

Dang CV. Therapeutic targeting of Myc-reprogrammed cancer cell metabolism. Cold Spring Harb Symp Quant Biol. 2011; 76:369–374. [PubMed: 21960526]

Dang CV. MYC on the path to cancer. Cell. 2012; 149:22–35. [PubMed: 22464321]

Dang CV. MYC, metabolism, cell growth, and tumorigenesis. Cold Spring Harb Perspect Med. 2013; 3:a014217. [PubMed: 23906881]

Diolaiti D, McFerrin L, Carroll PA, Eisenman RN. Functional interactions among members of the MAX and MLX transcriptional network during oncogenesis. Biochim Biophys Acta. 2014

Du J, Cleghorn W, Contreras L, Linton JD, Chan GC, Chertov AO, Saheki T, Govindaraju V, Sadilek M, Satrustegui J, et al. Cytosolic reducing power preserves glutamate in retina. Proc Natl Acad Sci U S A. 2013; 110:18501–18506. [PubMed: 24127593]

Du P, Kibbe WA, Lin SM. lumi: a pipeline for processing Illumina microarray. Bioinformatics. 2008; 24:1547–1548. [PubMed: 18467348]

Duran RV, Oppliger W, Robitaille AM, Heiserich L, Skendaj R, Gottlieb E, Hall MN. Glutaminolysis activates Rag-mTORC1 signaling. Mol Cell. 2012; 47:349–358. [PubMed: 22749528]

Eberlin LS, Gabay M, Fan AC, Gouw AM, Tibshirani RJ, Felsher DW, Zare RN. Alteration of the lipid profile in lymphomas induced by MYC overexpression. Proc Natl Acad Sci U S A. 2014; 111:10450–10455. [PubMed: 24994904]

Eischen CM, Roussel MF, Korsmeyer SJ, Cleveland JL. Bax loss impairs Myc-induced apoptosis and circumvents the selection of p53 mutations during Myc-mediated lymphomagenesis. Mol Cell Biol. 2001; 21:7653–7662. [PubMed: 11604501]

Eisen MB, Spellman PT, Brown PO, Botstein D. Cluster analysis and display of genome-wide expression patterns. Proc Natl Acad Sci U S A. 1998; 95:14863–14868. [PubMed: 9843981]

Evan GI, Wyllie AH, Gilbert CS, Littlewood TD, Land H, Brooks M, Waters CM, Penn LZ, Hancock DC. Induction of apoptosis in fibroblasts by c-myc protein. Cell. 1992; 69:119–128. [PubMed: 1555236]

Feng Z, Levine AJ. The regulation of energy metabolism and the IGF-1/mTOR pathways by the p53 protein. Trends Cell Biol. 2010; 20:427–434. [PubMed: 20399660]

Gao P, Tchernyshyov I, Chang TC, Lee YS, Kita K, Ochi T, Zeller KI, De Marzo AM, Van Eyk JE, Mendell JT, et al. c-Myc suppression of miR-23a/b enhances mitochondrial glutaminase expression and glutamine metabolism. Nature. 2009; 458:762–765. [PubMed: 19219026]

Griffiths B, Lewis CA, Bensaad K, Ros S, Zhang Q, Ferber EC, Konisti S, Peck B, Miess H, East P, et al. Sterol regulatory element binding protein-dependent regulation of lipid synthesis supports cell survival and tumor growth. Cancer Metab. 2013; 1:3. [PubMed: 24280005]

Han KS, Ayer DE. MondoA senses adenine nucleotides: transcriptional induction of thioredoxin-interacting protein. Biochem J. 2013; 453:209–218. [PubMed: 23631812]

Hooker CW, Hurlin PJ. Of Myc and Mnt. J Cell Sci. 2006; 119:208–216. [PubMed: 16410546]

Huang da W, Sherman BT, Lempicki RA. Systematic and integrative analysis of large gene lists using DAVID bioinformatics resources. Nat Protoc. 2009; 4:44–57. [PubMed: 19131956]

Huang M, Weiss WA. Neuroblastoma and MYCN. Cold Spring Harb Perspect Med. 2013; 3:a014415. [PubMed: 24086065]

Hubert CG, Bradley RK, Ding Y, Toledo CM, Herman J, Skutt-Kakaria K, Girard EJ, Davison J, Berndt J, Corrin P, et al. Genome-wide RNAi screens in human brain tumor isolates reveal a novel viability requirement for PHF5A. Genes Dev. 2013; 27:1032–1045. [PubMed: 23651857]

Janoueix-Lerosey I, Lequin D, Brugieres L, Ribeiro A, de Pontual L, Combaret V, Raynal V, Puisieux A, Schleiermacher G, Pierron G, et al. Somatic and germline activating mutations of the ALK kinase receptor in neuroblastoma. Nature. 2008; 455:967–970. [PubMed: 18923523]

Kaadige MR, Looper RE, Kamalanaadhan S, Ayer DE. Glutamine-dependent anapleurosis dictates glucose uptake and cell growth by regulating MondoA transcriptional activity. Proc Natl Acad Sci U S A. 2009; 106:14878–14883. [PubMed: 19706488]

Kim SS, Shago M, Kaustov L, Boutros PC, Clendening JW, Sheng Y, Trentin GA, Barsyte-Lovejoy D, Mao DY, Kay R, et al. CUL7 is a novel antiapoptotic oncogene. Cancer Res. 2007; 67:9616–9622. [PubMed: 17942889]

Leithner K, Hrzenjak A, Trotzmuller M, Moustafa T, Kofeler HC, Wohlkoenig C, Stacher E, Lindenmann J, Harris AL, Olschewski A, et al. PCK2 activation mediates an adaptive response to glucose depletion in lung cancer. Oncogene. 2014

Li F, Wang Y, Zeller KI, Potter JJ, Wonsey DR, O'Donnell KA, Kim JW, Yustein JT, Lee LA, Dang CV. Myc stimulates nuclearly encoded mitochondrial genes and mitochondrial biogenesis. Mol Cell Biol. 2005; 25:6225–6234. [PubMed: 15988031]

Lin CY, Loven J, Rahl PB, Paranal RM, Burge CB, Bradner JE, Lee TI, Young RA. Transcriptional amplification in tumor cells with elevated c-Myc. Cell. 2012; 151:56–67. [PubMed: 23021215]

Link JM, Ota S, Zhou ZQ, Daniel CJ, Sears RC, Hurlin PJ. A critical role for Mnt in Myc-driven T-cell proliferation and oncogenesis. Proc Natl Acad Sci U S A. 2012; 109:19685–19690. [PubMed: 23150551]

Lopez-Bigas N, Cline M, Broom B, Margolin A, Omberg L, Weinstein J, MA. Thread 4: Data discovery, transparency and visualization. Nature Genetics. 2013; 45

Lutz W, Stohr M, Schurmann J, Wenzel A, Lohr A, Schwab M. Conditional expression of N-myc in human neuroblastoma cells increases expression of alpha-prothymosin and ornithine decarboxylase and accelerates progression into S-phase early after mitogenic stimulation of quiescent cells. Oncogene. 1996; 13:803–812. [PubMed: 8761302]

McFerrin LG, Atchley WR. Evolution of the Max and Mlx networks in animals. Genome Bio Evol. 2011; 3:915–937. [PubMed: 21859806]

McFerrin LG, Atchley WR. A novel N-terminal domain may dictate the glucose response of Mondo proteins. PLoS One. 2012; 7:e34803. [PubMed: 22506051]

Mendez-Lucas A, Hyrossova P, Novellasdemunt L, Vinals F, Perales JC. Mitochondrial Phosphoenolpyruvate Carboxykinase (PEPCK-M) Is a Pro-survival, Endoplasmic Reticulum (ER) Stress Response Gene Involved in Tumor Cell Adaptation to Nutrient Availability. J Biol Chem. 2014; 289:22090–22102. [PubMed: 24973213]

Meroni G, Cairo S, Merla G, Messali S, Brent R, Ballabio A, Reymond A. Mlx, a new Max-like bHLHZip family member: the center stage of a novel transcription factors regulatory pathway? Oncogene. 2000; 19:3266–3277. [PubMed: 10918583]

Metallo CM, Gameiro PA, Bell EL, Mattaini KR, Yang J, Hiller K, Jewell CM, Johnson ZR, Irvine DJ, Guarente L, et al. Reductive glutamine metabolism by IDH1 mediates lipogenesis under hypoxia. Nature. 2012; 481:380–384. [PubMed: 22101433]

Morrish F, Noonan J, Perez-Olsen C, Gafken PR, Fitzgibbon M, Kelleher J, VanGilst M, Hockenbery D. Myc-dependent mitochondrial generation of acetyl-CoA contributes to fatty acid biosynthesis and histone acetylation during cell cycle entry. J Biol Chem. 2010; 285:36267–36274. [PubMed: 20813845]

Nicklin P, Bergman P, Zhang B, Triantafellow E, Wang H, Nyfeler B, Yang H, Hild M, Kung C, Wilson C, et al. Bidirectional transport of amino acids regulates mTOR and autophagy. Cell. 2009; 136:521–534. [PubMed: 19203585]

Nie Z, Hu G, Wei G, Cui K, Yamane A, Resch W, Wang R, Green DR, Tessarollo L, Casellas R, et al. c-Myc is a universal amplifier of expressed genes in lymphocytes and embryonic stem cells. Cell. 2012; 151:68–79. [PubMed: 23021216]

O'Shea JM, Ayer DE. Coordination of nutrient availability and utilization by MAX- and MLX-centered transcription networks. Cold Spring Harb Perspect Med. 2013; 3:a014258. [PubMed: 24003245]

Oberthuer A, Berthold F, Warnat P, Hero B, Kahlert Y, Spitz R, Ernestus K, Konig R, Haas S, Eils R, et al. Customized oligonucleotide microarray gene expression-based classification of neuroblastoma patients outperforms current clinical risk stratification. J Clin Oncol. 2006; 24:5070–5078. [PubMed: 17075126]

Peterson CW, Stoltzman CA, Sighinolfi MP, Han KS, Ayer DE. Glucose controls nuclear accumulation, promoter binding, and transcriptional activity of the MondoA-Mlx heterodimer. Mol Cell Biol. 2010; 30:2887–2895. [PubMed: 20385767]

Qing G, Li B, Vu A, Skuli N, Walton ZE, Liu X, Mayes PA, Wise DR, Thompson CB, Maris JM, et al. ATF4 regulates MYC-mediated neuroblastoma cell death upon glutamine deprivation. Cancer Cell. 2012; 22:631–644. [PubMed: 23153536]

Sans CL, Satterwhite DJ, Stoltzman CA, Breen KT, Ayer DE. MondoA-Mlx heterodimers are candidate sensors of cellular energy status: mitochondrial localization and direct regulation of glycolysis. Mol Cell Biol. 2006; 26:4863–4871. [PubMed: 16782875]

Shachaf CM, Perez OD, Youssef S, Fan AC, Elchuri S, Goldstein MJ, Shirer AE, Sharpe O, Chen J, Mitchell DJ, et al. Inhibition of HMGcoA reductase by atorvastatin prevents and reverses MYC-induced lymphomagenesis. Blood. 2007; 110:2674–2684. [PubMed: 17622571]

Sloan EJ, Ayer DE. Myc, mondo, and metabolism. Genes Cancer. 2010; 1:587–596. [PubMed: 21113411]

Sridharan R, Tchieu J, Mason MJ, Yachechko R, Kuoy E, Horvath S, Zhou Q, Plath K. Role of the murine reprogramming factors in the induction of pluripotency. Cell. 2009; 136:364–377. [PubMed: 19167336]

Stoltzman CA, Peterson CW, Breen KT, Muoio DM, Billin AN, Ayer DE. Glucose sensing by MondoA:Mlx complexes: a role for hexokinases and direct regulation of thioredoxin-interacting protein expression. Proc Natl Acad Sci U S A. 2008; 105:6912–6917. [PubMed: 18458340]

Szabo C, Coletta C, Chao C, Modis K, Szczesny B, Papapetropoulos A, Hellmich MR. Tumor-derived hydrogen sulfide, produced by cystathionine-beta-synthase, stimulates bioenergetics, cell proliferation, and angiogenesis in colon cancer. Proc Natl Acad Sci U S A. 2013; 110:12474–12479. [PubMed: 23836652]

Tong X, Zhao F, Mancuso A, Gruber JJ, Thompson CB. The glucose-responsive transcription factor ChREBP contributes to glucose-dependent anabolic synthesis and cell proliferation. Proc Natl Acad Sci U S A. 2009; 106:21660–21665. [PubMed: 19995986]

Vander Heiden MG, Cantley LC, Thompson CB. Understanding the Warburg effect: the metabolic requirements of cell proliferation. Science. 2009; 324:1029–1033. [PubMed: 19460998]

Wang H, Hammoudeh DI, Follis AV, Reese BE, Lazo JS, Metallo SJ, Prochownik EV. Improved low molecular weight Myc-Max inhibitors. Mol Cancer Ther. 2007; 6:2399–2408. [PubMed: 17876039]

Wang Q, Diskin S, Rappaport E, Attiyeh E, Mosse Y, Shue D, Seiser E, Jagannathan J, Shusterman S, Bansal M, et al. Integrative genomics identifies distinct molecular classes of neuroblastoma and shows that multiple genes are targeted by regional alterations in DNA copy number. Cancer Res. 2006; 66:6050–6062. [PubMed: 16778177]

Wasylishen AR, Kalkat M, Kim SS, Pandyra A, Chan PK, Oliveri S, Sedivy E, Konforte D, Bros C, Raught B, et al. MYC activity is negatively regulated by a C-terminal lysine cluster. Oncogene. 2013; 33:1066–1072. [PubMed: 23435422]

Wernicke CM, Richter GH, Beinvogl BC, Plehm S, Schlitter AM, Bandapalli OR, Prazeres da Costa O, Hattenhorst UE, Volkmer I, Staege MS, et al. MondoA is highly overexpressed in acute lymphoblastic leukemia cells and modulates their metabolism, differentiation and survival. Leuk Res. 2012; 36:1185–1192. [PubMed: 22748921]

Wise DR, DeBerardinis RJ, Mancuso A, Sayed N, Zhang XY, Pfeiffer HK, Nissim I, Daikhin E, Yudkoff M, McMahon SB, et al. Myc regulates a transcriptional program that stimulates mitochondrial glutaminolysis and leads to glutamine addiction. Proc Natl Acad Sci U S A. 2008; 105:18782–18787. [PubMed: 19033189]

Xia J, Mandal R, Sinelnikov IV, Broadhurst D, Wishart DS. MetaboAnalyst 2.0--a comprehensive server for metabolomic data analysis. Nucleic Acids Res. 2012; 40:W127–133. [PubMed: 22553367]

Yuneva M, Zamboni N, Oefner P, Sachidanandam R, Lazebnik Y. Deficiency in glutamine but not glucose induces MYC-dependent apoptosis in human cells. J Cell Biol. 2007; 178:93–105. [PubMed: 17606868]

Yuneva MO, Fan TW, Allen TD, Higashi RM, Ferraris DV, Tsukamoto T, Mates JM, Alonso FJ, Wang C, Seo Y, et al. The metabolic profile of tumors depends on both the responsible genetic lesion and tissue type. Cell Metab. 2012; 15:157–170. [PubMed: 22326218]

Zaidi N, Lupien L, Kuemmerle NB, Kinlaw WB, Swinnen JV, Smans K. Lipogenesis and lipolysis: the pathways exploited by the cancer cells to acquire fatty acids. Prog Lipid Res. 2013; 52:585–589. [PubMed: 24001676]

Zhang J, Grubor V, Love CL, Banerjee A, Richards KL, Mieczkowski PA, Dunphy C, Choi W, Au WY, Srivastava G, et al. Genetic heterogeneity of diffuse large B-cell lymphoma. Proc Natl Acad Sci U S A. 2013; 110:1398–1403. [PubMed: 23292937]

Zhang P, Metukuri MR, Bindom SM, Prochownik EV, O'Doherty RM, Scott DK. c-Myc is required for the CHREBP-dependent activation of glucose-responsive genes. Mol Endocrinol. 2010; 24:1274–1286. [PubMed: 20382893]

Significance

Altered cellular metabolism is recognized as a hallmark of cancer. Understanding how cells modify their metabolism to promote tumorigenesis is critical for the development of effective therapeutic strategies to specifically target cancer cells. Activation of the oncogene *MYC* facilitates proliferation through metabolic reprogramming; however, the contribution of the larger Myc transcriptional network to tumorigenesis remains to be explored. Here we show that deregulated Myc is dependent on the related network members MondoA and Mlx. The glucose-responsive transcription factor MondoA/Mlx enables Myc-driven glutamine addiction and facilitates the reprogramming of cancer cell metabolism while attenuating Myc-induced stress. This report identifies a role of the extended transcriptional network in regulating Myc's oncogenic functions and may lead to future anti-Myc therapeutic opportunities.
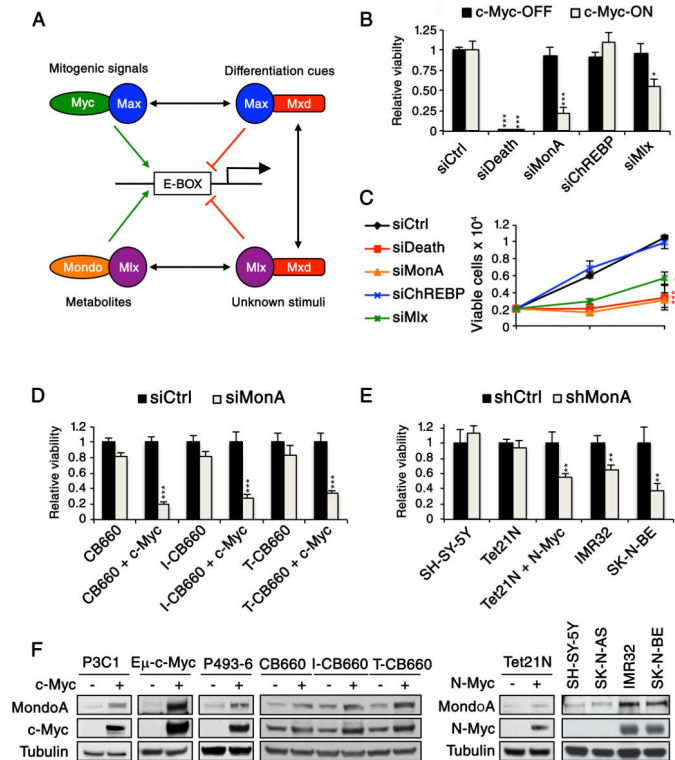
Figure 1. Synthetic Lethal dependency of deregulated Myc on MondoA

(A) Simplified Myc network schematic showing competition for heterodimerization partners (black lines with double arrowhead) and genomic E-Box loci between network members (green and red lines indicate transcriptional activation and repression, respectively). **(B–E)** Relative viability of P3C1 (B), CB660 and its immortalized (I-CB660) or Ras-transformed (T-CB660) derivatives (D), or neuroblastoma (E) cell lines or cell number of P493-6 cells (C) transfected with indicated siRNAs normalized to the corresponding non-silencing control (siCtrl). A pro-apoptotic siRNA mix (siDeath) is included as a positive control for transfection efficiency. Shown are mean and SD (n=3). **(F)** Western blot analysis for MondoA, c-Myc and N-Myc across the indicated cell lines under indicated conditions. See also Figure S1 and Table S1.
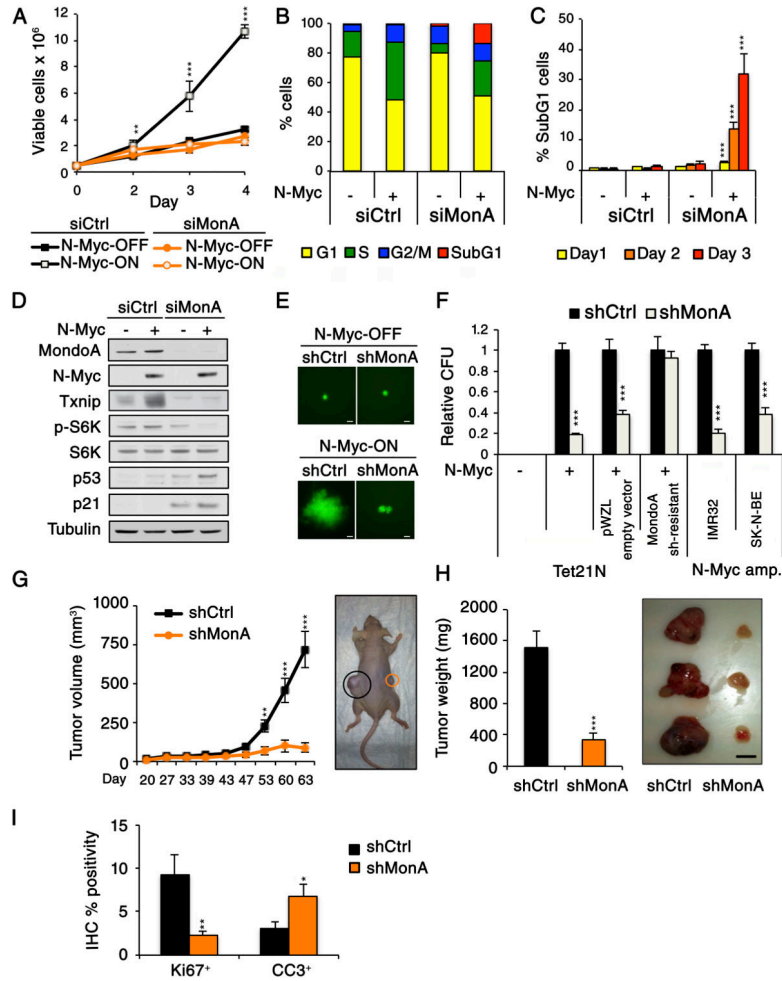
Figure 2. Loss of MondoA blocks N-Myc-induced proliferation and tumorigenesis while potentiating apoptosis both in vitro and in vivo
(**A**) Growth curves of Tet21N cells, with or without N-Myc overexpression, treated with either siCtrl or siMonA. Shown are mean and SD, n=3. (**B**) Cell cycle analysis of cells from panel A at day 3. (**C**) Time course quantification of sub-G1 cell population. Shown are mean and SD, (n=3). (**D**) Western Blot analysis for the indicated proteins in Tet21N cells with or without N-Myc overexpression at day 3 post-transfection of either siCtrl or siMonA. (**E, F**) Representative colony morphology (E) and quantification of colony formation (F) of neuroblastoma cells in soft agar at day 14 after plating. Scale bar = 20 μm. CFU: Colony-forming units. Shown are mean and SEM, (n=9). (**G**) Subcutaneous growth of Tet21N cells stably expressing either shCtrl or shMonA in Nu/Nu mice and a representative animal at end point. (**H**) Final tumor weight and representative image of tumors at end point. For (G–H) Shown are mean and SEM (n=10). Scale bar = 1 cm. (**I**) Quantification of immunohistochemistry positivity for Ki67 and cleaved-caspase 3 (CC3) in tumors from (G) Shown are mean and SEM (n=12). See also Figure S2.
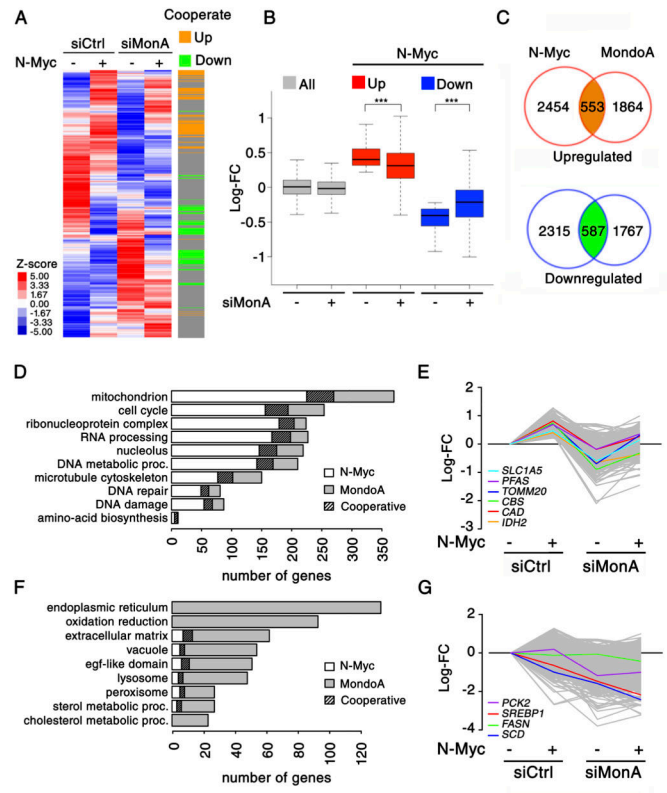
Figure 3. Transcriptional coordination between N-Myc and MondoA regulates metabolism and proliferation

(**A**) Heatmap generated by TreeView representing the median Z-score of all genes whose expression is altered for each condition. (**B**) Log fold change (Log-FC) of all, N-Myc upregulated, and N-Myc downregulated probes in the presence or absence of MondoA. Shown is a box plot indicating maximum (upper line), 3rd quartile (top of box), median (line in box), 1st quartile (bottom of box) and minimum (lower line). (**C**) Venn diagram of N-Myc (in the presence of MondoA) and MondoA (in the presence of N-Myc) regulated genes. (**D**) Gene Ontology (GO) Analysis: genes upregulated by N-Myc (white), MondoA (grey) or both (striped) for each category are shown. (**E**) Global expression profile of N-Myc and MondoA cooperatively upregulated genes among the four conditions. Genes encoding metabolic regulator as indicated with colored lines. (**F**) GO analysis of MondoA regulated genes (N-Myc-ON condition) (**G**) Global expression profile of MondoA upregulated genes involved in lipid and glucose metabolism as indicated with colored lines. See also Figure S3.
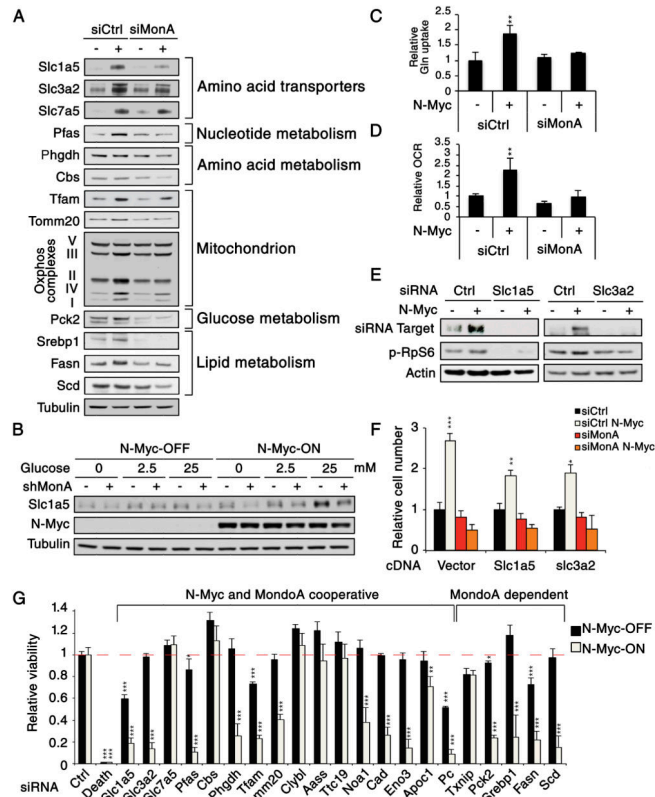
Figure 4. N-Myc and MondoA coordinately regulate metabolic and mitochondrial targets in Tet21N cells

(A) Western blot analysis of a subset of N-Myc and MondoA coordinately regulated or MondoA-dependent targets. **(B)** Western blot analysis of Tet21N cells under the indicated conditions in response to glucose stimulation. **(C)** Glutamine (Gln) uptake assay of Tet21N cells with the indicated treatment. Shown are mean and SD, n=3. **(D)** Oxygen consumption rate (OCR) assay of Tet21N cells with the indicated treatment. Shown are mean and SD (n=3). **(E)** Western blot analysis of the indicated proteins in siCtrl cells or cells with KD of Slc1A5 or Slc3A2. **(F)** Cells expressing indicated proteins or vector control were transfected with siCtrl or siMonA and viable cells were enumerated by trypan blue exclusion after 4 days. Shown are mean and SD, n=3. **(G)** Viability of cells in the presence or absence of Myc expression (normalized to the relative control siRNA) 4 days after transfection with the indicated siRNA. Shown are mean and SD (n=3). The red line indicates the control is set to 1. See also Figure S4 and Table S1.
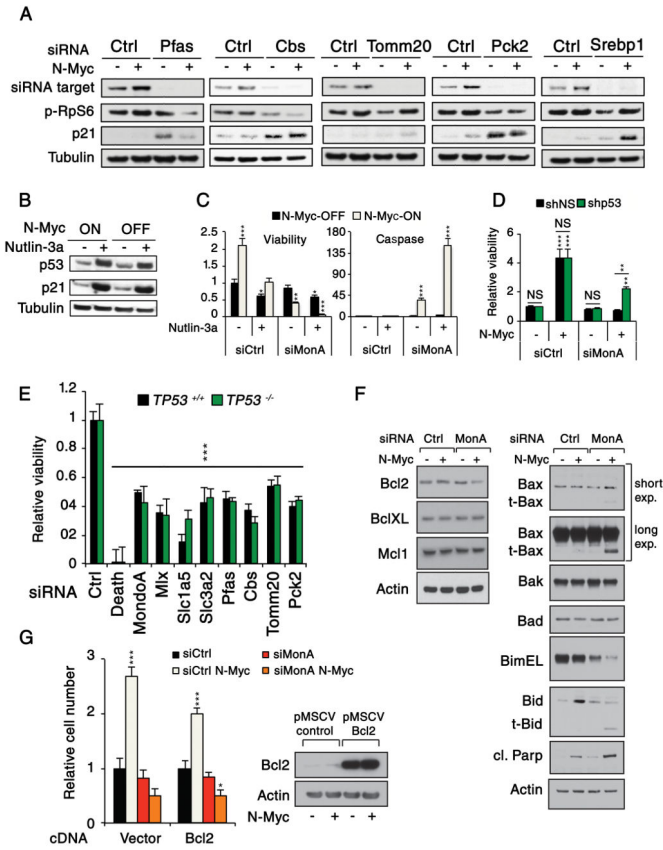
Figure 5. MondoA suppresses N-Myc-induced metabolic stress

(**A**) Western blot analysis of Tet21N under the indicated conditions transfected with the indicated siRNA. (**B**) Western blot analysis of Tet21N cells for the indicated proteins (−/+ N-Myc and −/+ nutlin-3a). (**C**) Cell viability (Cell Titer Glo) and apoptosis (Caspase-Glo Reagent) quantification after nutlin-3a treatment under the indicated conditions. Shown are mean and SEM (n=5). (**D**) Viability assay of Tet21N cells expressing either a control or a p53 shRNA. Shown are mean and SD (n=3). (**E**) Viability assay of HCT116 p53$^{+/+}$ and p53$^{−/−}$ cells after knockdown of MondoA, Mlx and Myc/MondoA target genes. Shown are mean and SEM (n=5). (**F**) Western blot analysis of the indicated apoptosis-related proteins in the Tet21N cells (−/+ N-Myc) under siCtrl or siMonA treatment. (**G**) Tet21N cells (−/+ N-Myc) expressing vector control (same as in Figure 4F) or BCL2 were transfected with siCtrl or siMonA and viable cells were enumerated by trypan blue exclusion after 4 days (left) and Western blot for Bcl2. Shown are mean and SD (n=3). See also Figure S6.

Figure 6. Metabolomic profiling of N-Myc and MondoA regulated pathways

(A) Heatmap depicting normalized and log-transformed metabolomic survey of 139 soluble metabolites under the four conditions. Color code for bar graphs in (A–E), white: siCtrl, blue: siCtrl+N-Myc, green: siMonA, and orange: siMonA+N-Myc. **(B)** Metabolite Set Enrichment Analysis (MSEA) of metabolite data from each condition compared to siCtrl. Shown is the −Log p Value for enrichment with a 0.05 p value indicated by the red line at 1.34. **(C)** GC-MS tracing of $^{13}C_5$-Gln for 24 hr in the Tet21N cells (−/+N-Myc) with siCtrl or siMonA treatment with the quantification of the mass isotopomers downstream of Gln indicated. Shown is mean and SD (n=3). **(D)** Quantification of total citrate (Cit) as in (C), normalized to relative cell number. Shown is mean and SD (n=3). **(E)** GC-MS tracing of $^{13}C_5$-Gln for 48 hr in the Tet21N cells as in (C), with contribution of $^{13}C_5$-Gln-derived acetyl-coA to palmitate indicated by m+(2n) isotopomers. The de novo fatty acid synthesis pathway is indicated, with enzymes shown in blue. Shown is mean and SD (n=3). **(F)** Relative caspase activity of Tet21N cells (−/+N-Myc) transfected with siCtrl or siMonA for 24 hr then treated with vehicle control (NT), ZOL, or C75 for 48 hr was measured by Caspase-Glo reagent. Shown is mean and SEM (n=5). **(G)** Tet21N cells were transfected with the indicated siRNA and treated with either vehicle (BSA), BSA+GGOH or BSA-conjugated Oleate 24 hr post-transfection and viability was assessed by Cell-Titer Glo reagent at 96 hr. Shown is mean and SEM (n=5). **(H)** Western blot analysis of cells treated

as in (G) for the indicated proteins. All p values were calculated by ANOVA. See also Figure S6 and Table S2.
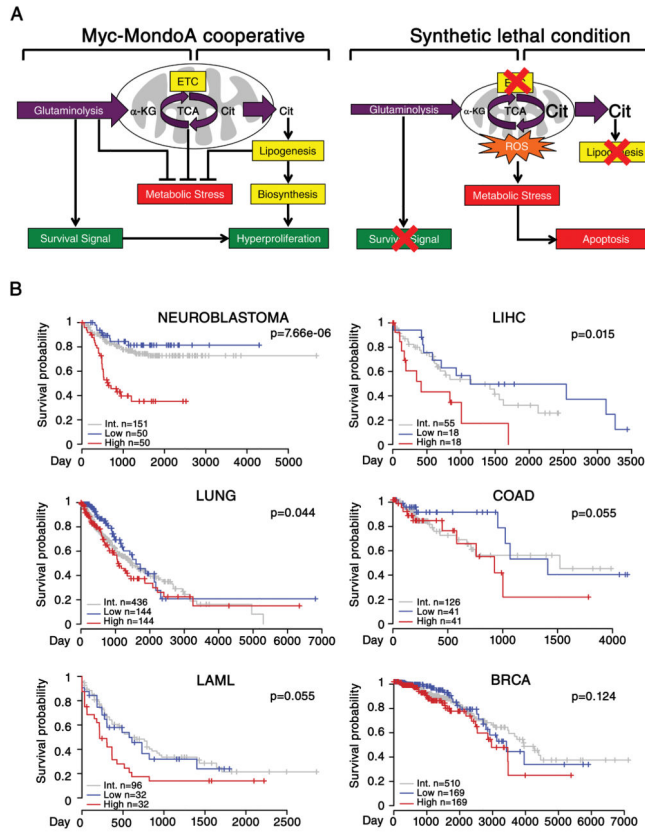
Figure 7. High expression of N-Myc and MondoA co-regulated metabolic genes correlates with poor prognosis

(A) Model of Myc-MondoA cooperation in regulation of cellular metabolism (left). Synthetic lethal condition upon activation of Myc and MondoA loss of function (right). Abbreviations: electron transport chain (ETC), tricarboxylic acid cycle (TCA) and reactive oxygen species (ROS). **(B)** Kaplan-Meier survival analysis based on the expression of selected Myc and MondoA-regulated genes. Red, blue and grey lines indicate the survival probability of patient with high (top 20%), low (bottom 20%) and intermediate (remaining 60%) cumulative expression of *MLXIP*, *CAD*, *TFAM*, *CBS*, *SCD*, *PFAS*, *SLC3A2*, and *SLC1A5*, respectively. Significance between the top and bottom 20% was determined by Wilcoxon model. Liver hepatocellular carcinoma (LIHC), lung squamous cell carcinoma and lung adenocarcinoma datasets combined (LUNG), colon adenocarcinoma (COAD), acute myeloid leukemia (LAML), and breast invasive carcinoma (BRCA). Gene datasets: neuroblastoma (Oberthuer 2006) and for rest, TCGA (http://cancergenome.nih.gov).